Supporting Information

Iversen et al. 10.1073/pnas.1407457111

SI Materials and Methods

Mass Spectrometry. Samples were run by using a Waters HDX-Manager with a desalting flow provided by an Agilent 1260 Infinity quaternary pump and a gradient flow provided by a nanoAcquity UPLC Binary Solvent Manager (Waters). For measurements on intact proteins (global-exchange analysis), a 50 μL/min gradient flow [5% (vol/vol) B to 50% B over 3 min] was used, along with a MassPREP Micro Desalting Column (Waters) for desalting. For measurements on peptides (local-exchange analysis), a 40 μL/min gradient flow (5% B to 50% B over 12 min) was used, along with ACQUITY UPLC BEH C18, 1.7 μm, 2.1 mm × 50 mm VanGuard Pre-Columns and 1.0 mm × 100 mm analytical columns for desalting and peptide separation, respectively. A column containing immobilized pepsin was placed between the loop and the desalting trap to digest the samples. Samples were subjected to electrospray ionization-MS by using a Waters Synapt G1 mass spectrometer with detector MCP voltage of 1,700 V for intact proteins or 1,950 V for peptides. Rigorous washing steps were performed between each injection.

Data Analysis. Mass spectra of intact TG2 were deconvoluted by using MaxEnt 1 in MassLynx v4.1. Peptides from peptic digests were identified from data-dependent acquisition MS/MS runs by using ProteinLynx Global Server v2.4 (Waters) and MassAI v1.05 (MassAI Bioinformatics, www.massai.dk). Deuterium incorporation for intact proteins and peptides was quantified by using DynamX v1.0 (Waters). Visualizations (PDB ID codes 2Q3Z and 1KV3) were created by using VMD v1.9.1 (1).

1. Humphrey W, Dalke A, Schulten K (1996) VMD: Visual molecular dynamics. *J Mol Graph* 14(1):33–38, 27-38.

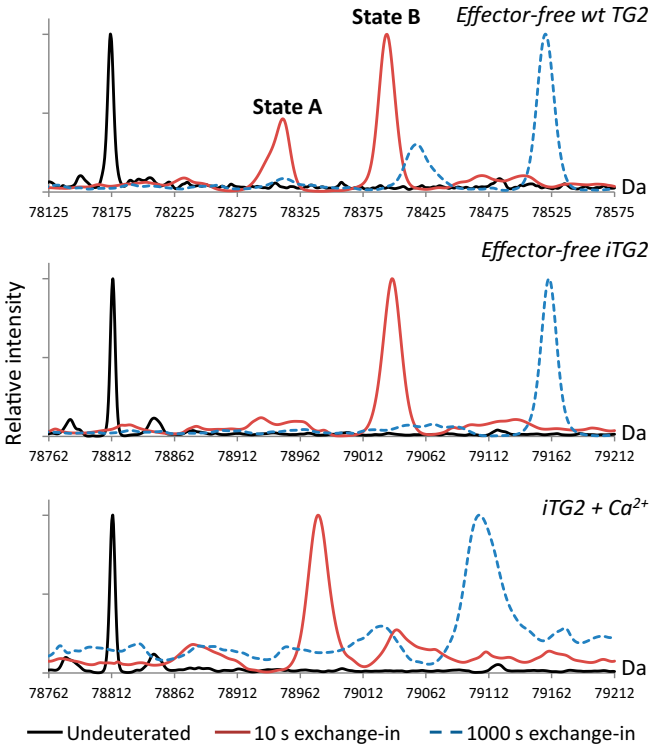

Fig. S1. Deconvoluted global-exchange spectra for effector-free WT TG2, effector-free iTG2, and iTG2 labeled in the presence of 5 mM $CaCl_2$. In the absence of Ca^{2+}, iTG2 and the open conformation, state B, in WT TG2 were found to exhibit similar behavior during isotopic exchange, indicating that the inhibitor had a minimal impact on the dynamics of the open conformation. The inhibitor did appear, however, to prevent the formation of closed conformation, state A. Adding Ca^{2+} to the solution before labeling had a pronounced stabilizing effect on iTG2.

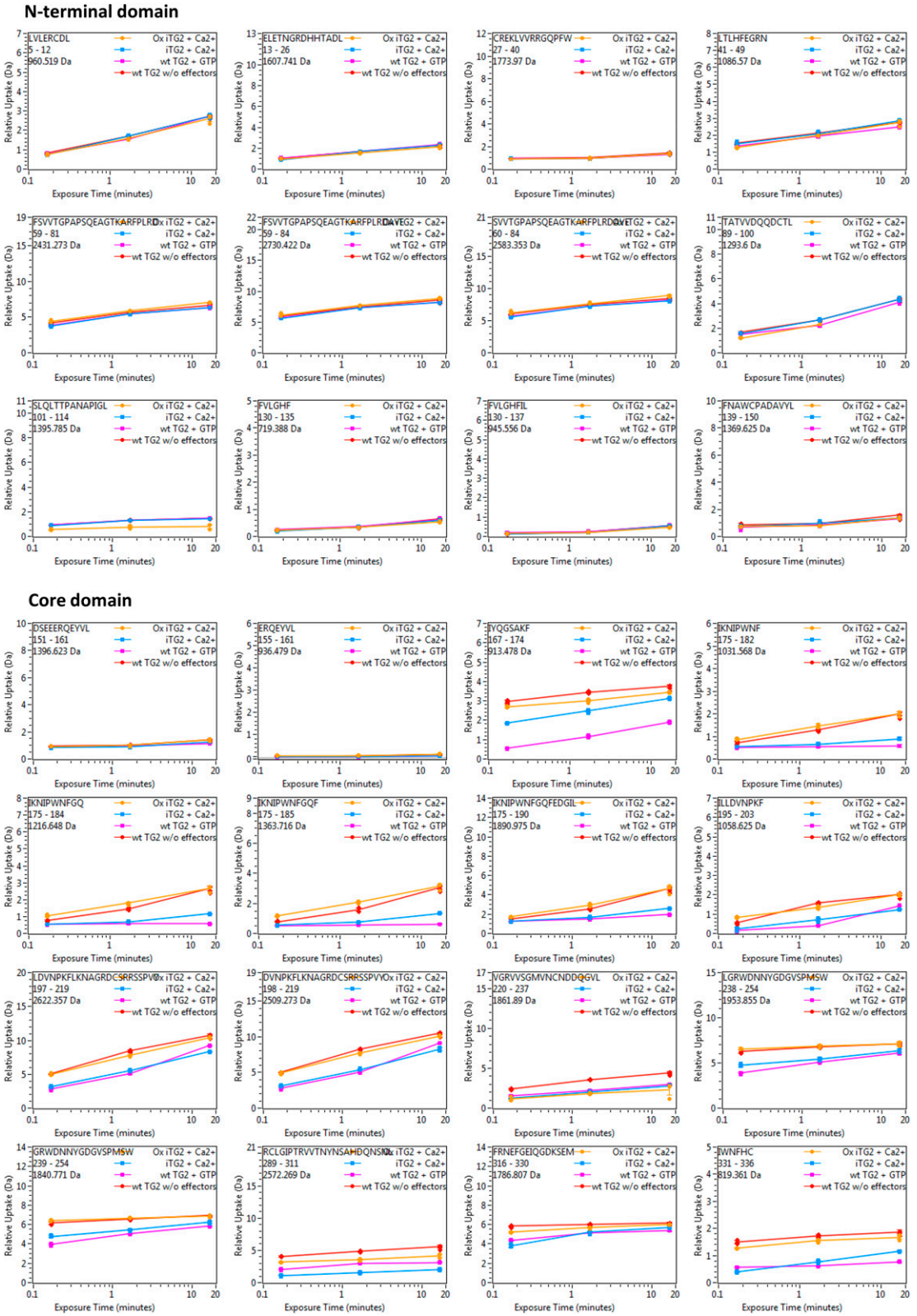

Fig. S2. (Continued)

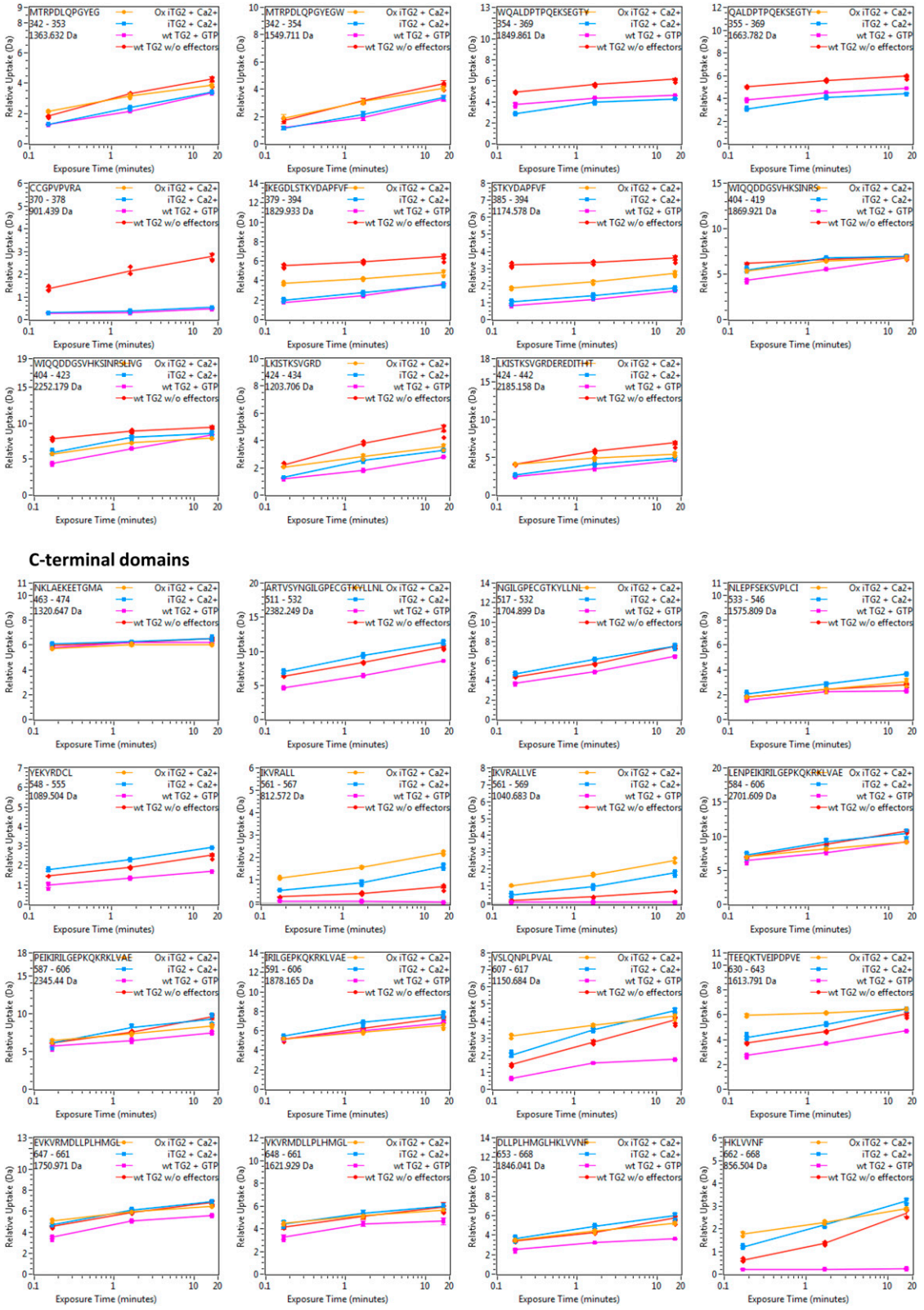

Fig. S2. Deuterium uptake plots for peptides located in the N-terminal, core, and C-terminal domains of TG2. Error bars represent SD based on labeling triplicates.

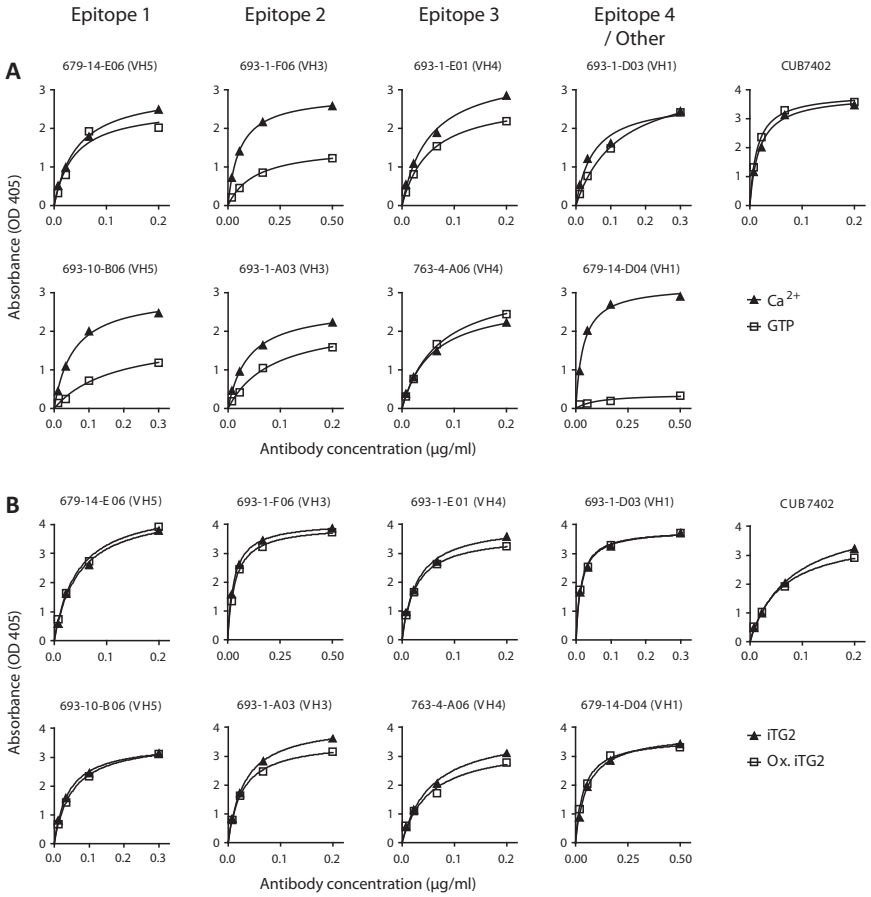

Fig. S3. Saturation binding curves showing reactivity of mAbs targeting different epitopes to TG2 subjected to various treatments in ELISA. The human mAbs have been assigned to epitopes 1–4 or "other" (1). The mouse mAb CUB7402, which targets a linear epitope, was included as a control that should give the same signal irrespective of TG2 conformation. (*A*) Comparison of mAb reactivity to Ca^{2+}-bound iTG2 and GTP-bound TG2. (*B*) Comparison of mAb reactivity to nonoxidized, Ca^{2+}-bound iTG2, and iTG2 that was oxidized before Ca^{2+} treatment.

1. Iversen R, et al. (2013) Transglutaminase 2-specific autoantibodies in celiac disease target clustered, N-terminal epitopes not displayed on the surface of cells. *J Immunol* 190(12): 5981–5991.

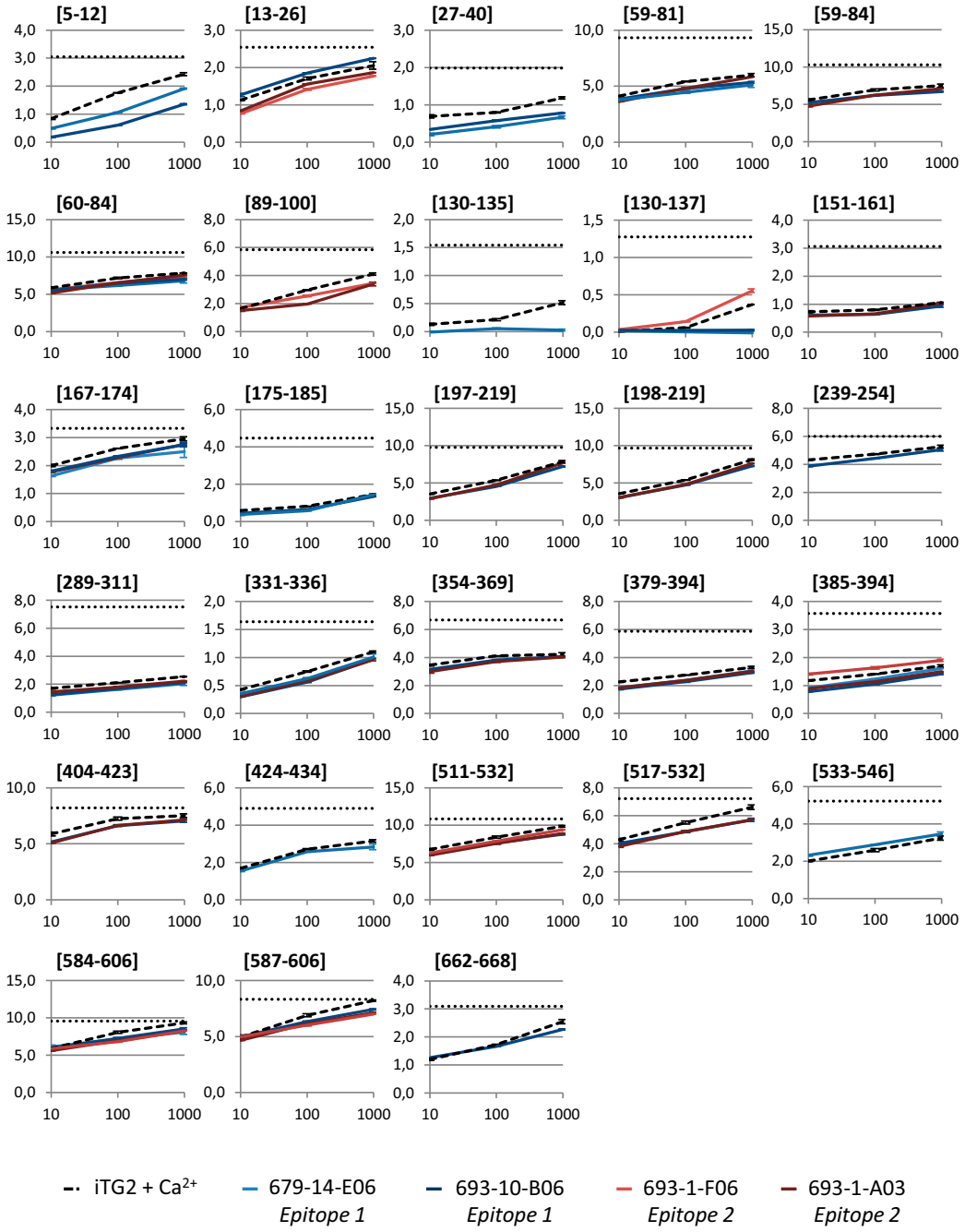

Fig. S4. Deuterium uptake plots for TG2 peptides, which exhibit a change in deuterium uptake upon antibody binding. Ca^{2+}-bound iTG2 was incubated in the presence or absence of TG2-specific mAbs before labeling. Exchange time, in seconds, is shown on the *x* axis, and deuterium uptake is shown on the *y* axis. For clarity, uptake plots for TG2–mAb complexes, which did not result in altered deuterium uptake, are not shown. Dotted horizontal lines represent the observed deuterium uptake in a full-deuteration control. Error bars represent SD based on analytical duplicates of a single labeling. For each peptide, all shown TG2–mAb complexes were found to exhibit a different deuterium uptake than unbound TG2 in at least two of three data points, based on unpaired two-tailed *t* tests ($P < 0.05$).

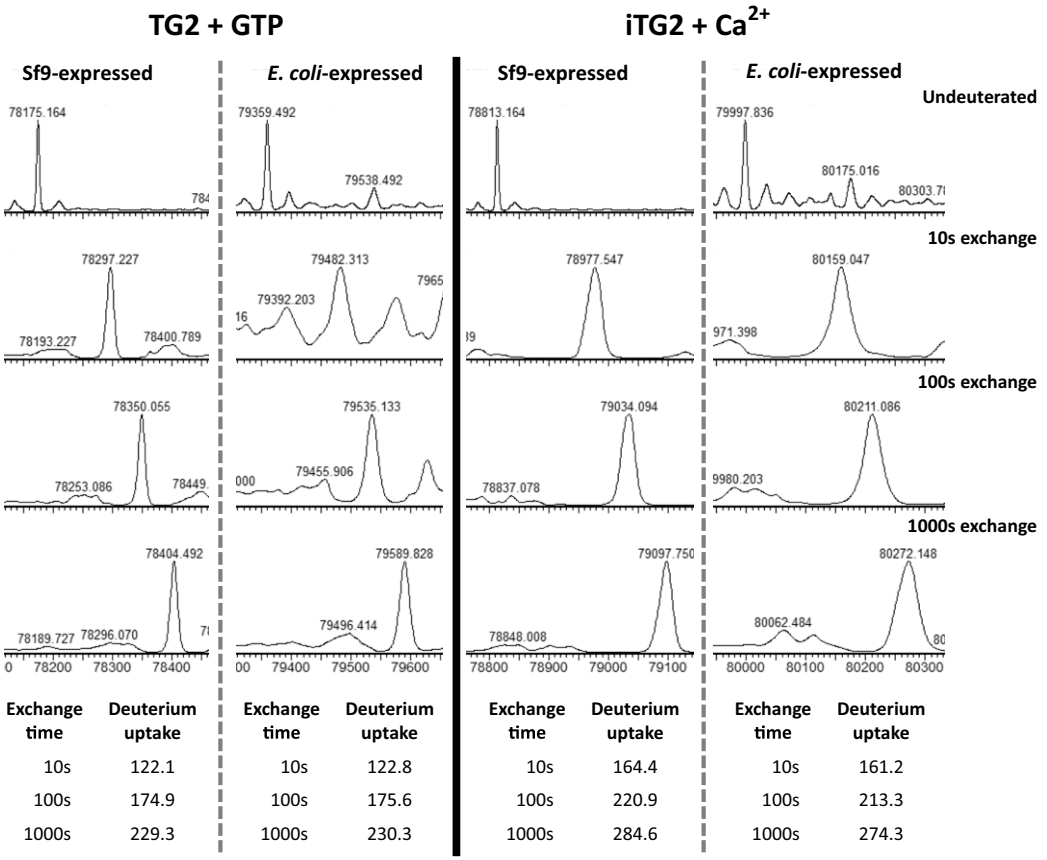

Exchange time	Deuterium uptake	Exchange time	Deuterium uptake	Exchange time	Deuterium uptake	Exchange time	Deuterium uptake
10s	122.1	10s	122.8	10s	164.4	10s	161.2
100s	174.9	100s	175.6	100s	220.9	100s	213.3
1000s	229.3	1000s	230.3	1000s	284.6	1000s	274.3

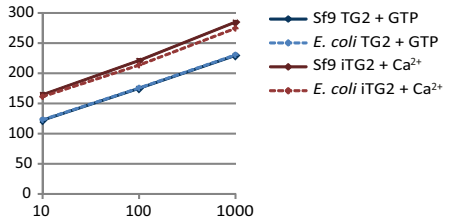

Fig. S5. Comparison of the deuterium uptake by TG2 produced in different expression systems. Recombinant human TG2 was either expressed in Sf9 insect cells or in *E. coli*. The two proteins contain slightly different purification tags (1), causing *E. coli*-produced TG2 to have a higher mass than the Sf9-produced enzyme. Deconvoluted mass spectra for GTP-bound TG2 and Ca^{2+}-bound iTG2, before deuteration and after 10-, 100-, and 1,000-s exchange, are shown. The corresponding values for deuterium uptake are shown in tables and displayed in a deuterium uptake plot. The two TG2 preparations exhibit very similar deuterium uptake, indicating that there are no major differences in their folding. Note that the absolute deuterium uptake values shown here are greater than those displayed in Table S1. This difference is due to these data being recorded at a later date, using an optimized analytical workflow.

1. Iversen R, et al. (2013) Transglutaminase 2-specific autoantibodies in celiac disease target clustered, N-terminal epitopes not displayed on the surface of cells. *J Immunol* 190(12): 5981–5991.

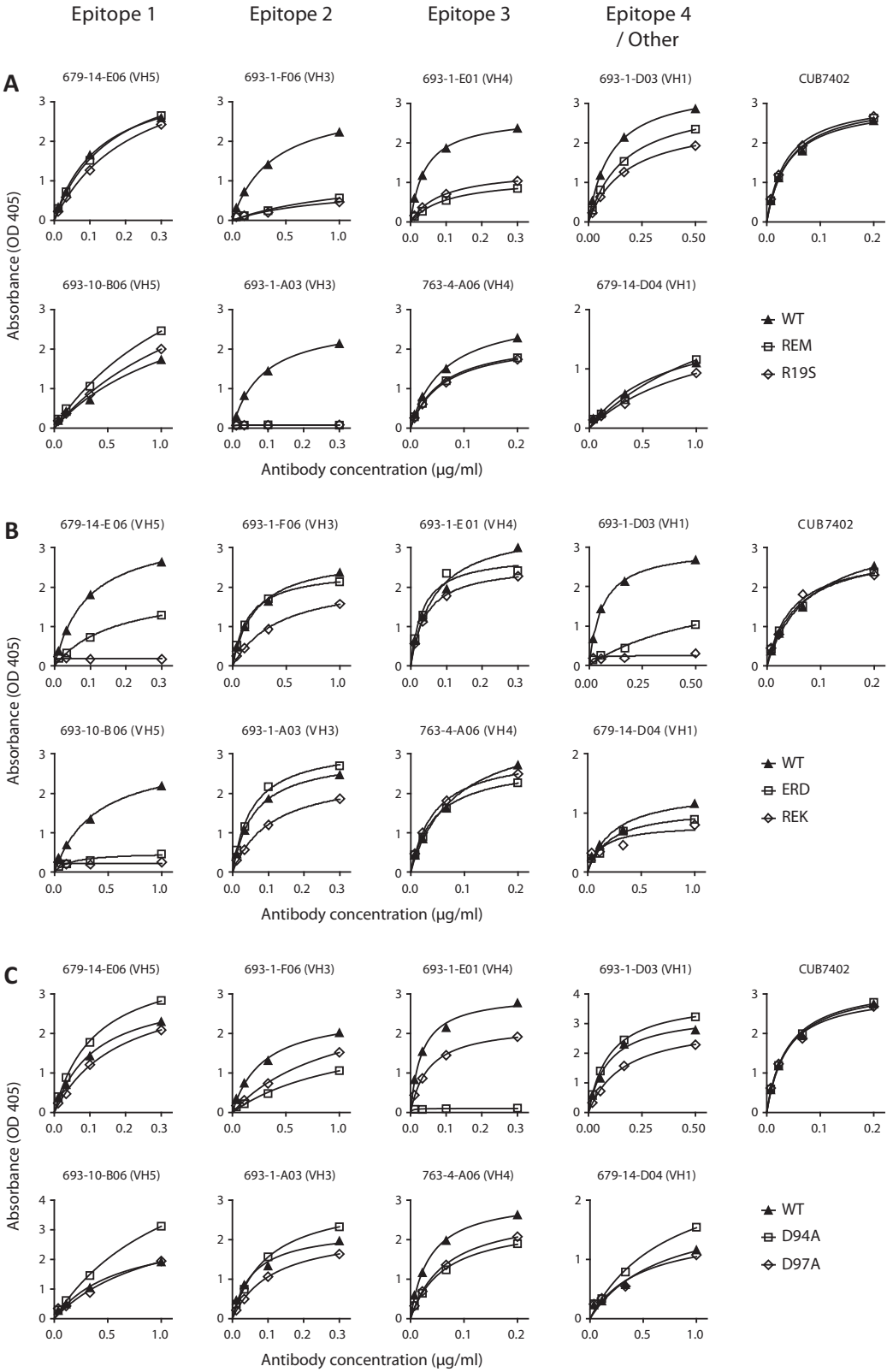

Fig. S6. Saturation binding curves showing the effect of introduced mutations on mAb binding to TG2 in ELISA. mAbs targeting different epitopes were tested for binding to WT and mutant TG2. The TG2-reactive mouse mAb CUB7402 was included as a control for equal coating of the TG2 variants. (*A*) Comparison of mAb reactivity to WT TG2, the R19S E153S M659S (REM) triple mutant, and R19S TG2. (*B*) Comparison of mAb reactivity to WT TG2 and the triple mutants E8Q R9S D11N (ERD) and R28S E29Q K30E (REK). The mutants were constructed based on the sequence of the homologous protein TG3, which is not recognized by the mAbs (1). (*C*) Comparison of mAb reactivity to WT, D94A, and D97A TG2.

1. Iversen R, et al. (2013) Transglutaminase 2-specific autoantibodies in celiac disease target clustered, N-terminal epitopes not displayed on the surface of cells. *J Immunol* 190(12):5981–5991.

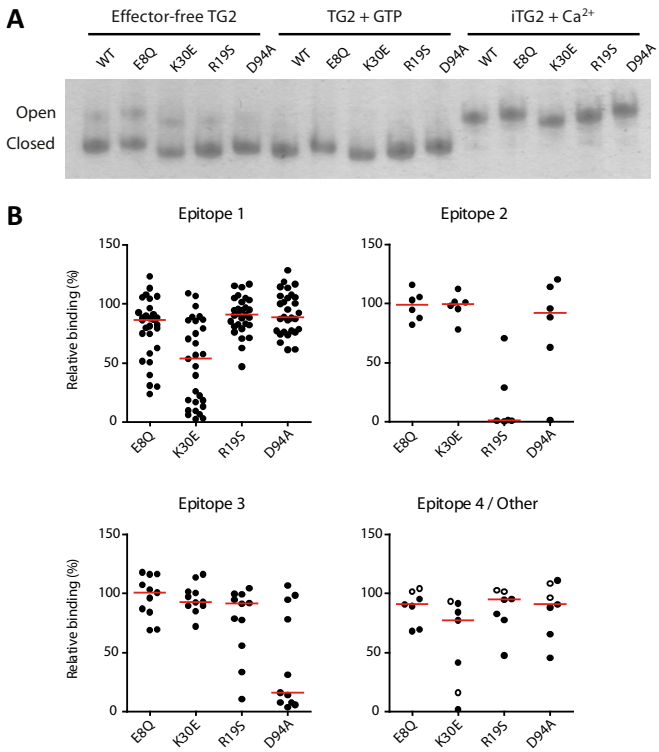

Fig. S7. Effect of TG2 mutations on protein conformation and binding to mAbs in the presence of Ca^{2+}. (*A*) Nondenaturing PAGE analysis of WT and mutant TG2 that had either been left untreated or incubated with GTP or a combination of Ca^{2+} and the active-site inhibitor Ac-P(DON)LPF-NH_2. WT and mutants display the same distributions between open and closed conformations. (*B*) Reactivity of 53 TG2-specific mAbs to mutant iTG2 in the presence of Ca^{2+} as determined by ELISA. Signals obtained with the indicated mutants are given relative to the signals obtained with WT iTG2. Red bars indicate medians. Compared with the results reported in Fig. 4, the mutations have lower impact on the binding of several mAbs when Ca^{2+} is present.

Table S1. Deuterium uptake in different TG2 states

Exchange time, s	State A	State B	TG2 + GTP	iTG2 + Ca^{2+}
10	118.6 (± 2.6)	189.4 (± 1.1)	116.8 (± 2.1)	142.0 (± 0.7)
100	161.6 (± 3.0)	240.6 (± 1.6)	157.1 (± 0.3)	191.5 (± 1.3)
1,000	204.9 (± 5.9)	293.1 (± 2.5)	197.1 (± 0.9)	236.3 (± 3.6)

Values represent the mass increase in daltons ± SD based on analytical duplicates of a single labeling.

Table S2. List of detected TG2 peptides and labeling characteristics

Peptide list			Effector binding*			Effect of oxidation*		
Start	End	Sequence	Protected when closed	Protected when open	All states similar	More dynamic when oxidized	Eff-free similar to Ox but not Red iTG2 w. Ca^{2+}	Effects upon mAb binding†
N-terminal domain								
5	12	LVLERCDL			X			X
13	26	ELETNGRDHHTADL			X			X
27	40	CREKLVVRRGQPFW			X			X
41	49	LTLHFEGRN			X			
59	81	FSVVTGPAPSQEAGTKARFPLRD			X			X
59	84	FSVVTGPAPSQEAGTKARFPLRDAVE			X			X
60	84	SVVTGPAPSQEAGTKARFPLRDAVE			X			X
89	100	TATVVDQQDCTL			X			X
101	114	SLQLTTPANAPIGL			X			
130	135	FVLGHF			X			X
130	137	FVLGHFIL			X			X
139	150	FNAWCPADAVYL			X			
Core domain								
151	161	DSEEERQEYVL			X			X
155	161	ERQEYVL			X			
167	174	IYQGSAKF	X			X	X	X
175	182	IKNIPWNF	X			X	X	
175	184	IKNIPWNFGQ	X			X	X	
175	185	IKNIPWNFGQF	X			X	X	X
175	190	IKNIPWNFGQFEDGIL	X			X	X	
195	203	ILLDVNPKF				X	X	
197	219	LDVNPKFLKNAGRDCSRRSSPVY				X	X	X
198	219	DVNPKFLKNAGRDCSRRSSPVY				X	X	X
220	237	VGRVVSGMVNCNDDQGVL						
238	254	LGRWDNNYGDGVSPMSW	X			X	X	
239	254	GRWDNNYGDGVSPMSW	X			X	X	X
289	311	RCLGIPTRVVTNYNSAHDQNSNL		X		X		X
316	330	FRNEFGEIQGDKSEM				X	X	
331	336	IWNFHC	X			X	X	X
342	353	MTRPDLQPGYEG				X	X	
342	354	MTRPDLQPGYEGW				X	X	
354	369	WQALDPTPQEKSEGTY		X		Ox data NA‡	Ox data NA‡	X
355	369	QALDPTPQEKSEGTY		X		Ox data NA‡	Ox data NA‡	
370	378	CCGPVPVRA				Ox data NA‡	Ox data NA‡	
379	394	IKEGDLSTKYDAPFVF				X		X
385	394	STKYDAPFVF				X		X
404	419	WIQQDDGSVHKSINRS	X					
404	423	WIQQDDGSVHKSINRSLIVG	X					X
424	434	LKISTKSVGRD	X			X		X
424	442	LKISTKSVGRDEREDITHT				X		
C-terminal domains								
463	474	NKLAEKEETGMA			x			
511	532	ARTVSYNGILGPECGTKYLLNL	X			Ox data NA‡	Ox data NA‡	X
517	532	NGILGPECGTKYLLNL	X			Ox data NA‡	Ox data NA‡	X
533	546	NLEPFSEKSVPLCI	X					X
548	555	YEKYRDCL	X			Ox data NA‡	Ox data NA‡	
561	567	IKVRALL	X					
561	569	IKVRALLVE	X					
584	606	LENPEIKIRILGEPKQKRKLVAE	X					X
587	606	PEIKIRILGEPKQKRKLVAE	X					X
591	606	IRILGEPKQKRKLVAE	X					
607	617	VSLQNPLPVAL	X					
630	643	TEEQKTVEIPDPVE	X					
647	661	EVKVRMDLLPLHMGL	X					
648	661	VKVRMDLLPLHMGL	X					
653	668	DLLPLHMGLHKLVVNF	X					
662	668	HKLVVNF	X					X

*Color coding matches the one used in Fig. 2 on the open and closed structures of TG2. Deuterium uptake plots, which the identifications are based on, are shown in Fig. S2.

†For the indicated peptides, deuterium uptake was found to be significantly different upon mAb binding, based on unpaired two-tailed t tests ($P < 0.05$). The relevant deuterium uptake plots are shown in Fig. S4.

‡Peptides could not be observed in the oxidized samples. Cysteine residues present in these peptides or at the pepsin cleavage site have presumably formed disulfide bonds.